IMPROVING DEEP POLICY GRADIENTS WITH VALUE FUNCTION SEARCH

Anonymous authors
Paper under double-blind review

ABSTRACT

Deep Policy Gradient algorithms employ value networks to drive the learning of parameterized policies and reduce the variance of the gradient estimates. However, value function approximation gets stuck in local optima and struggles to fit the actual return, limiting the variance reduction efficacy and leading policies to sub-optimal performance. In this paper, we focus on improving value approximation and analyzing the effects on Deep Policy Gradient primitives such as value prediction, variance reduction, and correlation of gradient estimates with the true gradient. To this end, we introduce a Value Function Search that employs a population of perturbed value networks to search for a better approximation. Our framework does not require additional environment interactions, gradient computations, or ensembles, providing a computationally inexpensive approach to enhance the supervised learning task on which value networks train. Crucially, we show that improving Deep Policy Gradient primitives results in improved sample efficiency and policies with higher returns using standard policy gradient methods on common continuous control benchmark domains.

1 INTRODUCTION

Deep Policy Gradient (PG) methods achieved impressive results in numerous control tasks (Schulman et al., 2017; Haarnoja et al., 2018; Fujimoto et al., 2018). However, such methods deviate from the underlying theoretical framework to compute gradients tractably. Hence, the promising performance of Deep PG algorithms suggests a lack of rigorous analysis to motivate such results. In this direction, Ilyas et al. (2020) empirically investigated the phenomena arising in practical Deep PG implementations by taking a closer look at key PG primitives such as gradient estimates and value predictions. Interestingly, the learned value networks used for predictions (*critics*) poorly fit the actual return. As a result, the local optima where critics get stuck limits their efficacy in the gradient estimates, driving policies (*actors*) toward sub-optimal performance.

Despite the lack of empirical investigations to understand Deep PG's results, several approaches have been proposed to improve these methods over the years. Ensemble learning (Wiering & van Hasselt, 2008; Lee et al., 2021; He et al., 2022), for example, combines multiple learning actors' (or critics') predictions to address overestimation and foster diversity. As such, these methods generate different solutions that improve exploration and stabilize the training, leading to higher returns. However, the number of models used at training and inference time poses significant challenges that we discuss in Section 5. Nonetheless, popular Deep Reinforcement Learning (RL) algorithms (e.g., Twin Delayed Deep Deterministic Policy Gradient (TD3) (Fujimoto et al., 2018)) leverage two value networks to improve robustness and performance, leveraging the benefits of ensemble approaches while limiting their complexity. To address the issues of ensembles, gradient-free population-based approaches have been recently proposed (Khadka & Tumer, 2018; Marchesini et al., 2021; Sigaud, 2022). The underlying idea is to complement Deep PG algorithms with a periodical policy search mechanism that relies on a population of perturbed policies to improve exploration and to find policy parameters that lead to higher payoffs (i.e., *better* policies). In contrast to ensemble methods that employ multiple actors and critics, gradient-free population searches typically focus on the actors, disregarding the value network component of Deep PG. Section 5 discusses the limitations of such policy search methods in detail.

However, in a PG context, critics have a pivotal role in driving the policy learning process as

poor value predictions lead to sub-optimal performance, and higher variance in gradient estimates (Sutton & Barto, 2018). Such issues are further exacerbated in state-of-the-art Deep PG methods as they struggle to learn good value function estimation, as detailed by Ilyas et al. (2020). For this reason, we propose a novel gradient-free population-based approach for critics called Value Function Search (VFS), depicted in Figure 1. We aim to improve Deep PG algorithms by enhancing value networks to achieve (i) a better fit of the actual return, (ii) a higher correlation of the gradients estimate with the (approximate) true gradient, and (iii) reduced variance. In detail, given a Deep PG agent characterized by actor and critic networks, VFS periodically instantiates a population of perturbed critics using a two-scale perturbation noise designed to improve value predictions. Small-scale perturbations explore *local* value predictions that only slightly modify those of the original critic (similarly to gradient-based perturbations (Lehman et al., 2018; Martin H. & de Lope, 2009)). Big-scale perturbations search for parameters that allow escaping from local optima where value networks get stuck. In contrast to previous search methods, evaluating perturbed value networks require computing standard value error measures using samples from the agent's buffer. Hence, the Deep PG agent uses the parameters with the lowest error until the next periodical search. Crucially, VFS's critics-based design addresses the issues of prior methods as it does not require a simulator, hand-designed environment interactions, or weighted optimizations. Moreover, our population's goal is to find the weights that minimize the same objective of the Deep PG critic.

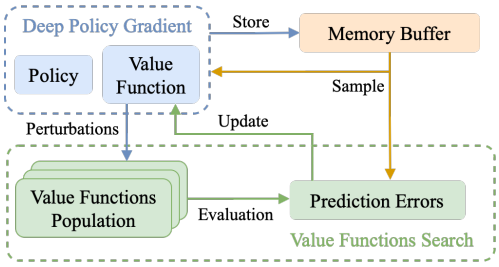

Figure 1: Overview of Value Function Search.

We show the effectiveness of VFS on different Deep PG baselines: (i) Proximal Policy Optimization (PPO) (Schulman et al., 2017), (ii) Deep Deterministic Policy Gradient (DDPG) (Lillicrap et al., 2016), and (iii) TD3 on a range of common continuous control benchmark tasks (Brockman et al., 2016; Todorov et al., 2012). We compare over such baselines, an ensembled Deep RL method, SUNRISE (Lee et al., 2021), and the policy search Supe-RL (Marchesini et al., 2021). In addition, we analyze key Deep PG primitives (i.e., value prediction errors, gradient estimate, and variance) to motivate the performance improvement of VFS-based algorithms. Our evaluation confirms that VFS leads to better gradient estimates with a lower variance that significantly improve sample efficiency and lead to policies with higher returns. Our analysis highlights a fundamental issue with current state-of-the-art Deep PG methods, opening the door for future research in this area.

2 Background

PG methods parameterize a policy π_θ with a parameters vector θ (typically the weights of a Deep Neural Network (DNN) in a Deep PG context), and $\pi_\theta(a_t|s_t)$ models the probability to take action a_t in a state s_t at step t in the environment. These approaches aim to learn θ following the gradient of an objective η_θ over such parameters (Sutton & Barto, 2018). Formally, the primitive gradient estimate on which modern Deep PG algorithms build has the following form (Sutton et al., 1999):

$$\nabla\eta_\theta = \mathbb{E}_{(s_t,a_t)\in\tau\sim\pi_\theta}\left[\nabla_\theta \log\pi_\theta(a_t|s_t) Q_{\pi_\theta}(s_t,a_t)\right] \tag{1}$$

where $(s_t, a_t) \in \tau \sim \pi_\theta$ are states and actions that form the trajectories sampled from the distribution induced by π_θ, and $Q_{\pi_\theta}(s_t, a_t)$ is the expected return after taking a_t in s_t. However, Equation 1 suffers from high-variance expectation, and different baselines have been used to margin the issue. In particular, given a discount value $\gamma \in [0, 1)$, the state-value function $V_{\pi_\theta}(s)$ is an ideal baseline as it leaves the expectation unchanged while reducing variance (Williams, 1992):

$$V_{\pi_\theta}(s) = \mathbb{E}_{\pi_\theta}\left[G_t := \sum_{t}^{\infty}\gamma^t r_{t+1}|s_t = s\right] \tag{2}$$

where G_t is the sum of future discounted rewards (*return*). Despite building on the theoretical framework of PG, Deep PG algorithms rely on several assumptions and approximations for designing feasible updates for the policy parameters. In more detail, these methods typically build on surrogate objective functions that are easier to optimize. A leading example is TRPO (Schulman et al., 2015), which ensures that a surrogate objective updates the policy locally by imposing a trust

region. Formally, TRPO imposes a constraint on the Kullback–Leibler diverge (KL) on successive policies $\pi_\theta, \pi_{\theta'}$, resulting in the following optimization problem:

$$\max_\theta \mathbb{E}_{\pi_\theta}\left[\frac{\pi_\theta(a_t|s_t)}{\pi_{\theta'}(a_t|s_t)}A_{\pi_\theta}(s_t,a_t)\right] \text{ s.t. } D_{KL}(\pi_\theta(\cdot|s)||\pi_{\theta'}(\cdot|s)) \leq \delta \tag{3}$$

where δ is a hand-tuned divergence threshold, and $A(s,a) = Q(s,a) - V(s)$ is the advantage function. In practical implementations, Equation 3 is tractably optimized with additional tricks: (i) a second-order approximation of the objective, (ii) a mean KL of the current trajectory instead of the actual KL divergence. Given TRPO's computational demands, Schulman et al. (2017) further "relaxes" the optimization landscape by replacing the constraint with the following clipped objective, providing a significantly faster (i.e., less demanding) yet better-performing alternative over TRPO:[1]

$$\max_\theta \mathbb{E}_{\pi_\theta}\left[\min\left(\frac{\pi_\theta(a_t|s_t)}{\pi_{\theta'}(a_t|s_t)}A(s_t,a_t), \text{clip}\left(\frac{\pi_\theta(a_t|s_t)}{\pi_{\theta'}(a_t|s_t)}, 1-\epsilon, 1+\epsilon\right)A(s_t,a_t)\right)\right] \tag{4}$$

On a similar trend, Lillicrap et al. (2016) leverages the deterministic PG theorem (Silver et al., 2014) for learning deterministic policies $\mu_\theta(s)$. In more detail, DDPG and further optimizations (e.g., TD3) are tightly related to standard Q-learning (Watkins & Dayan, 1992) and assume having a differentiable action-value function over actions. Deterministic PG algorithms learn the value parameters as in standard Double DQN, while policy parameters are learned under the $\max_\theta \mathbb{E}_{\pi_\theta}\left[Q_\phi(s,\mu_\theta(s))\right]$ optimization problem, where ϕ are the parameters of the critic. Moreover, TD3 addresses the overestimation of DDPG with additional tricks, e.g., learning two value functions, being pessimistic about the action value to use for the target computation, and delaying the policy updates.

In summary, Deep PG algorithms build their practical success on learning value functions for driving the learning of the policy parameters θ. However, we argue that significant research efforts have been devoted to improving policies, as discussed in Section 1, while the attention to improving critics appears marginal. Hence, to our knowledge, VFS is the first gradient-free population-based approach that works on top of Deep PG to improve critics without facing the complexities of learning ensembles or policy searches.

2.1 Gradient-Informed Perturbations

Previous policy search approaches generate a population of perturbed versions of the agent's policy π_θ to explore variations with higher returns (Khadka & Tumer, 2018; Marchesini et al., 2021; Khadka et al., 2019; Colas et al., 2018; Sigaud, 2022). To this end, gradient-informed perturbations (or variations) have been employed for limiting detrimental effects on π_θ, exploring small changes in the population's action sampling process (Lehman et al., 2018; Marchesini et al., 2021). In more detail, prior methods express the average divergence of a policy at state s over a perturbation ω as:

$$d(\pi_\theta, \omega) = \|\pi_\theta(\cdot|s) - \pi_{\theta+\omega}(\cdot|s)\|_2 \tag{5}$$

and use the gradient of such divergence to approximate the sensitivity of θ over the policy decisions, which is used to normalize Gaussian-based perturbations. Formally, following Lehman et al. (2018):

$$\nabla_{\theta_a} d(\pi_\theta, \omega) \approx \nabla_\theta d(\pi_\theta, 0) + H_\theta(d(\pi_\theta, 0))\omega \tag{6}$$

where H_θ is the Hessian of divergence with respect to θ. Although simpler first-order approximations of Equation 6 achieve comparable results, gradient-based perturbations add significant overhead to the training process. Crucially, prior work introduced gradient-based variations because it is hard to evaluate the population against possible detrimental changes. As such, the quality of perturbed policies should be assessed over many trajectories to ensure that they effectively achieve higher returns over arbitrary environment initializations (Marchesini et al., 2021). In contrast to prior work, we focus on a critics-based search where high-scale perturbations may help the learning process to escape from local optima, achieving better predictions. Hence, VFS relies on a two-scale perturbation approach to maintain similar value predictions to the original value function while also exploring diverse parameters to escape from local optima.

[1] We do not consider the unconstrained penalty-based PPO due to the better performance of the clipped one.

3 VALUE FUNCTION SEARCH

We introduce a gradient-free population-based search with a two-scale perturbation method to enhance critics employed in Deep PG algorithms. Ultimately, we aim to show that value functions with better predictions are crucial to improve Deep PG primitives, leading to significantly better sample efficiency and policies with higher returns.

Algorithm 1 shows the general flow of the proposed Value Function Search framework. During a standard training procedure of a Deep PG agent, VFS periodically generates a population $\mathcal{P}$ of perturbed value networks, starting from the agent's current critic parametrized by ϕ. We first instantiate n copies of ϕ and two Gaussian noise distributions $\mathcal{G}_{\min,max}$ with $\sigma_{\min,max}$ standard deviation for the two-scale variations (lines 3-4). Hence, we sample from the two distributions to apply each perturbation to half of the population (lines 5-6). In contrast to single-scale or gradient-based perturbations of prior work (Khadka & Tumer, 2018; Marchesini et al., 2021; Sigaud, 2022), the two scales approach for value networks has the following advantages:[2] (i) $\mathcal{G}_{\min}$ maintains similar predictions to those of the unperturbed critic, similarly to gradient-based variations. Sampling from $\mathcal{N}(0, \sigma_{\min})$ translates into small changes in the value prediction process to find a better set of parameters within a local search fashion. (ii) $\mathcal{G}_{\max}$ is a Gaussian with a greater standard deviation $\mathcal{N}(0, \sigma_{\max})$ used to explore diverse value predictions, to escape from local optima. (iii) Gaussian-based perturbations do not introduce significant overhead as gradient-based variations. After generating the population, VFS samples a batch b of trajectories from the agent's buffer B. There are different strategies for sampling the required experiences from the agent's memory based on the nature of the Deep PG algorithm. When using an on-policy agent (e.g., TRPO, PPO), we apply VFS after updating the policy and value networks. In this way, we reuse the same on-policy data to evaluate whether a perturbed set of weights has better value prediction (i.e., lower error). Off-policy agents (e.g., DDPG, TD3) could also follow a similar strategy. Still, the reduced size of the mini-batches typically employed by off-policy updates would result in noisy evaluations. For this reason, we sample a larger batch of experiences to provide a more robust evaluation. In practice, to compute the prediction errors for each value network in the population (line 7), we use the typical objective used to train PG critics, the Mean Squared Error (MSE) (Sutton & Barto, 2018), whose general formulation is:

$$mse_{\phi_i}(b) = \frac{1}{|b|} \sum_{s \in b} \left[V_\pi(s) - V_{\pi_{\phi_i}}(s) \right]^2 \tag{7}$$

where $V_\pi(s)$ is the true value function (or a bootstrapped approximation). On-policy updates are particularly interesting, as Deep PG algorithms typically learn critics with Monte-Carlo methods without bootstrapping the target value. Hence, performing a supervised learning procedure on (s_t, G_t) pairs, where the return G_t is an unbiased, noisy sample of $V_\pi(s)$ that replaces the expectation of Equation 2 with an empirical average. We then refer to a perturbed critic as a *local* improvement of the original unperturbed one when it achieves a lower error on b. In our context, given a value network parametrized by ϕ, a batch of visited trajectories b, and a perturbation ω, we define the value network parametrized by $\phi+\omega$ to be a local improvement of ϕ when $mse_{\phi+\omega}(b) \leq mse_\phi(b)$. Moreover, in the limit where b samples all the trajectories, $G_t \equiv V_\pi(s_t)$, and $mse_{\phi+\omega}(b) \leq mse_\phi(b)$

Algorithm 1 Value Function Search

1: **Given:** (i) a Deep PG agent with a value network parametrized by ϕ at training epoch e; (ii) a buffer B of visited trajectories; (iii) periodicity e_s for VFS and population size n; (iv) scale $\sigma_{\min,\max}$ for the two-scale Gaussian noise $\mathcal{G}$.
2: **if** $e \,\%\, e_s = 0$ **then**
3: $\quad \mathcal{P} \leftarrow \{\phi_0, \ldots, \phi_n\}$ copies of ϕ
4: $\quad \mathcal{G}_{\min,\max} \leftarrow \mathcal{N}(0, \sigma_{\min,\max})$
5: $\quad \phi_{1:\frac{\lfloor P \rfloor}{2}} \leftarrow \phi_i + \mathcal{G}_{\min} \quad \phi_{\frac{\lfloor P \rfloor}{2}:n} \leftarrow \phi_i + \mathcal{G}_{\max}$
6: $\quad b \leftarrow$ Sample a batch of trajectories from B
7: $\quad mse_{\mathcal{P}} \leftarrow$ Evaluate $\mathcal{P}$ over b as Equation 7
8: $\quad \phi \leftarrow \min_{\phi_i \in \mathcal{P}} (mse_{\mathcal{P}})$
9: **end if**

[2]We support claims on our perturbation approach with additional experiments in Section 4.

means that $\phi + \omega$ is a better or equal fit of the true value function with respect to the original ϕ. Crucially, it is known that the Monte-Carlo value approximation converges to a local optimum even when using non-linear approximation (Sutton & Barto, 2018). Hence, on-policy VFS potentially maintains the same convergence guarantees of the chosen baseline.[3] To this end, it would be possible to employ annealing mechanisms for the perturbation scales (similar to the ones used for learning rates) to zero out the impact of VFS over the training phase. Hence, providing the diversity benefits of VFS early in the training while maintaining the convergence guarantee of the baseline algorithm within the limit. Nonetheless, as discussed in Ilyas et al. (2020), practical Deep PG algorithms deviate from the underlying theoretical framework, and we performed additional experiments in Section 4 to show that maintaining VFS through the entire learning process typically results in better performance over zeroing out the perturbations. In addition, in a worst-case scenario where the population search never improves the value prediction locally, VFS matches the same local optima of the original approach. However, following the insights of Fujimoto et al. (2018), practical Deep PG algorithms can not theoretically guarantee to reduce estimation errors or improve predictions outside the batch used for computing the update.

VFS addresses most limitations of previous policy search approaches and minimizes the same objective of the Deep PG critics, leading to the following crucial advantages:

- VFS does not require additional environment interactions or hand-designed evaluations for selecting the best set of parameters in the population.
- MSE is a widely adopted objective for learning value networks, providing an established evaluation strategy. Moreover, batch computations and parallelization make this process particularly efficient. Nonetheless, VFS is not specifically designed for MSE, and it is straightforward to extend it to different error measures.
- At the cost of adding overhead, the population evaluation may scale to an arbitrarily large number of samples to improve robustness.

Finally, the parameters with the lowest error replace the current agent's critic until the next population search (line 8). We note that many Deep RL algorithms employ target networks parametrized by ϕ_{tg} to reduce overestimation. In this scenario, we also update the target weights toward the new ones by using standard Polyak averaging with an $\alpha \in (0, 1)$ weight transfer value:

$$\phi_{tg} = \alpha\phi + (1 - \alpha)\phi_{tg} \tag{8}$$

3.1 Limitations

Here we highlight the limitations of VFS: (i) batched computations and parallelization do not avoid a marginal overhead induced by the population search. (ii) In an off-policy setting, VFS requires tuning the batch size for the error computation to balance the trade-off between computational demands and the quality of the evaluation. (iii) There are no guarantees that small-scale perturbations produce a local variation to the original predictions. However, they have been previously shown effective in doing so (Martin H. & de Lope, 2009), and we confirm this result in Section 4.

4 Experiments

The proposed experiments aim at answering the following questions: (i) How do VFS components affect the training phase. In particular, we investigate the efficacy of using $\sigma_{min,max}$ to maintain similar predictions and explore diversified ones, respectively, and when the perturbations are most effective during the training. (ii) How these components impact the performance and sample efficiency of VFS-based algorithms. (iii) How VFS influences Deep PG primitives, such as gradient estimates, their variance, and value predictions, to motivate the performance improvement.

We investigate the performance of VFS on the on-policy PPO (Schulman et al., 2017), the off-policy DDPG (Lillicrap et al., 2016), and TD3 (Fujimoto et al., 2018) algorithms. We compare over the baseline DDPG, PPO, TD3, SUNRISE (Lee et al., 2021) (a recent ensemble approach), and Supe-RL (Marchesini et al., 2021) (a recent policy search approach). We conduct our experiments on five

[3] Due to bootstrapping, the same result generally does not apply to temporal difference targets with non-linear function approximation.

Figure 2: Efficacy of the $\sigma_{min,max}$ scales in modifying PPO's critic to achieve similar predictions or more diversified ones to escape local optima, respectively. We observe the average difference (Δ) between values predicted by PPO's critic and its $\sigma_{min,max}$ variations over 100 episodes in the Hopper environment shown as different boxes.

common challenging continuous control tasks based on MuJoCo (Brockman et al., 2016), which are widely used for comparing Deep PG, ensembles, and policy search approach (Schulman et al., 2017; Lillicrap et al., 2016; Lee et al., 2021; Fujimoto et al., 2018; Marchesini et al., 2021).

Data are collected on nodes equipped with Xeon E5-2650 CPUs and 64GB of RAM, using the hyper-parameters reported in Appendix E. Considering reproducibility discussions and the importance of having statistically significant results (Colas et al., 2019; Henderson et al., 2018), we report the average performance of 25 runs per method, with shaded regions representing the standard error. Such a high number of experiments motivates slightly different results over the original implementations of DDPG, TD3, and PPO, referring to the original authors' results for Supe-RL and SUNRISE.

4.1 Analyzing VFS Components

The following analysis considers data collected in the Hopper environment and VFS-PPO, as we achieved comparable results in the other tasks and algorithms. Given the intuitions of Section 3, the two-scale perturbation approach has different effects on the Deep PG critic. We expect perturbation with σ_{min} to result in networks with similar predictions (i.e., values). In contrast, σ_{max} should generate networks with more diversified predictions to escape local optima. In this direction, Figure 2 shows the average difference between values predicted by the original critic of the PPO algorithm and its two perturbations (σ_{min} on the left, σ_{max} on the right) over 100 episodes (i.e., each box is an episode). In particular, we report the data collected in the initial stage of the training (i.e., at step 10^5), where green boxes indicate slight variations while red ones represent the highest difference in our evaluation. The values of the σ_{min} perturbed network differ from the original critic by a small margin. In contrast, the critic perturbed with σ_{max} achieves significantly different values. Hence, the proposed two-scale perturbation approach leads to the desired outcome, and σ_{min}-based variations confirm similar results over computationally demanding gradient-based perturbations. Such results are further confirmed in Appendix A, where we report the same evaluation in different stages of the training and for DDPG and TD3.

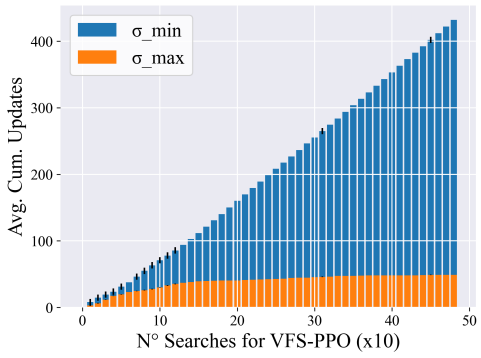

Figure 3: The average cumulative number of times when σ_{min} (blue) or σ_{max} (orange) variations improve the error of the Deep PG critic and the other perturbation.

Moreover, we expect critics with σ_{max} variations to be rarely better than σ_{min} variations and the original value network, as drastic changes in the value predictions serve to escape from local optima. To confirm this, Figure 3 shows the average cumulative number of times on which σ_{min} (blue) or σ_{max} (orange) critics' error is the lowest in the population compared to the original critic (y-axis),

Table 1: Performance at 1M steps for Hopper, Walker, Swimmer, and 2M steps for HalfCheetah, and Ant in PPO, DDPG, TD3 experiments. We show the average return and standard deviation over the 25 runs and the percentage of steps required by VFS methods to reach the peak performance of the corresponding baseline. For the policy search (Supe-RL) and the ensemble baseline (SUNRISE), we report the best number in prior works at 2×10^5 steps (Lee et al., 2021; Marchesini et al., 2021).

	PPO	**VFS-PPO**	
	Avg. Return		***Steps %***
Hopper	2287 ± 805	$\mathbf{2878 \pm 695}$	-48.5
Walker	2384 ± 1074	$\mathbf{2905 \pm 932}$	-12.4
Swimmer	80 ± 26	$\mathbf{86 \pm 22}$	-38.6
HalfCheetah	1756 ± 823	$\mathbf{2999 \pm 775}$	-65.7
Ant	1110 ± 353	$\mathbf{1545 \pm 333}$	-27.9

	DDPG	**VFS-DDPG**	
	Avg. Return		***Steps %***
Hopper	1734 ± 810	$\mathbf{2397 \pm 637}$	-34.9
Walker	1753 ± 858	$\mathbf{2492 \pm 755}$	-38.2
Swimmer	46 ± 2	$\mathbf{49 \pm 1}$	-36.1
HalfCheetah	7948 ± 2702	$\mathbf{9208 \pm 711}$	-45.4
Ant	427 ± 1177	$\mathbf{1667 \pm 565}$	-92.1

	TD3	**VFS-TD3**	
	Avg. Return		***Steps %***
Hopper	2558 ± 1029	$\mathbf{3185 \pm 398}$	-44.8
Walker	3773 ± 1052	$\mathbf{4185 \pm 860}$	-58.3
Swimmer	123 ± 27	$\mathbf{134 \pm 11}$	-34.0
HalfCheetah	10232 ± 1201	$\mathbf{12430 \pm 551}$	-58.3
Ant	3660 ± 1126	$\mathbf{4468 \pm 532}$	-40.8

	VFS-TD3	**Supe-RL**	**SUNRISE**
		Avg. Return	
Hopper	1216 ± 750	1024 ± 480	$\mathbf{2643 \pm 472}$
Walker	$\mathbf{2119} \pm 1054$	$1532 \pm \mathbf{946}$	1236 ± 1123
HalfCheetah	$\mathbf{6780} \pm 1017$	2087 ± 1132	$4501 \pm \mathbf{443}$
Ant	$\mathbf{1557} \pm \mathbf{447}$	1282 ± 214	1502 ± 483

over the periodical searches (x-axis). The linear growth of the σ_{min} bars indicates that such perturbations generally produce better variations over σ_{max} perturbations and the original critic through the training. In contrast, σ_{max} perturbed networks have more impact in the early stages of the training (where the critics' predictions are seldom accurate) and occasionally achieve lower error in later stages of the training, highlighting their role in VFS.

4.2 Empirical Evaluation

Here we discuss the performance and sample efficiency improvement of VFS-based algorithms. In particular, we discuss: (i) the average return at convergence and (ii) the percentage of samples required by VFS implementations to achieve the peak performance of the Deep PG baselines. Table 1 shows the results for PPO, VFS-PPO, DDPG, VFS-DDPG, TD3, and VFS-TD3 (the VFS-TD3 algorithm applies the value function search to both the critics employed by TD3). In each table, we highlight the highest average return in bold and refer to Appendix B for an exhaustive overview of the training curves. Generally, VFS-based algorithms achieve a significant performance improvement in average return and sample efficiency, confirming the benefits of improving critics during Deep PG training procedures. On average, VFS-PPO achieves a 33% return improvement and uses 38.6% fewer samples to reach the peak performance of PPO (i.e., it reaches PPO's peak return in -38.6% steps). VFS-DDPG has a 78% return improvement and 49.3% improvement in sample efficiency. Note that these results are biased by the poor performance of DDPG in the Ant task. Nonetheless, VFS-DDPG consistently outperforms the Deep PG baseline. We motivate such improvement due to the typical brittle convergence of DDPG, which is caused by the value overestimation that is addressed with VFS. Moreover, VFS-TD3 achieves an average 17.6% return improvement and 47.3% fewer samples to reach the peak performance of TD3. The latter results are particularly important as TD3 employs several tricks to address the poor performance of DDPG, and it is known to be a strong Deep PG baseline (Fujimoto et al., 2018). Nonetheless, VFS further improves its performance, especially the sample efficiency.

We compare VFS over the policy search Supe-RL and the ensemble method SUNRISE by considering their best number reported in prior works (Lee et al., 2021; Marchesini et al., 2021) at 2×10^5 steps (as in SUNRISE).[4] Crucially, the VFS implementation shows comparable or superior average performance over such additional baselines (75.6% and 17.9% on average, respectively), confirming the merits of our framework.

Finally, Appendix C contains: (i) additional experiments to show the effects of different population sizes on VFS-PPO; (ii) a comparison of the computational overhead for VFS, Supe-RL, and SUN-

[4]We do not consider the Swimmer environment as it has not being employed by prior work.

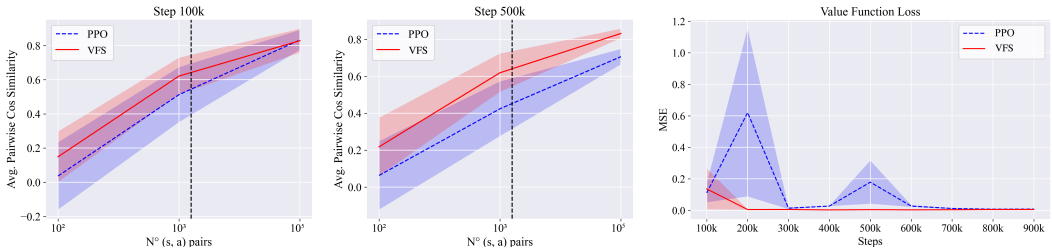

Figure 4: Analysis of gradient estimate and variance (left, middle) in the Hopper task for PPO and VFS-PPO. We measure the average pairwise cosine similarity (y-axis) between 30 gradient estimates which use a growing number of state-action pairs (x-axis). For each algorithm, we use the average over the 25 models collected during the training runs at 10^5 and 5×10^5 steps. The higher correlation with a lower variance of VFS-PPO translates into better performance of the Deep PG algorithm (Figure 1). Average MSE of such models over the training phase (right).

RISE that highlights the negligible overhead of VFS over such baselines; (iii) additional experiments to show that annealing variations have lower performance than the proposed VFS.

4.3 Deep PG Primitives Analysis

We analyze how VFS influences Deep PG primitives to motivate the performance improvement. To this end, Figure 4 left and middle show the quality of the gradient estimates and their variance at the initial and middle stages of the training (respectively), and the mean square error of PPO's critic and VFS-PPO one. Regarding gradient estimates, PPO's common implementations estimate the gradient using an empirical mean of $\approx 20^3$ samples (marked in the plots with a vertical line). Since the Deep PG agent successfully solves the task attaining high reward, these sample-based estimates are sufficient to drive successful learning of the policy parameters.

In particular, we measure the average pairwise cosine similarity and its standard deviation between 30 gradient measurements taken from the PPO and VFS-PPO models after 10^5 and 5×10^5 steps in the Hopper task with an increasing number of state-action pairs. Higher correlations mean that the gradient estimate is more similar to the actual gradient.[5] Following the PG's underlying theoretical framework, we also know that a lower variance in the gradient estimate typically translates into better performance, which is why value networks are employed in Deep PG. Crucially, VFS-PPO shows a higher correlation and lower variance in the sampling regime used during the training, motivating its performance improvement over the standard PPO. Moreover, Figure 4 on the right shows the average MSE of the 25 trained models for PPO and PPO-VFS computed every 10^5 step. Our results show that critics enhanced with VFS consistently result in lower MSE, which leads to the previously discussed improvements in the gradient estimates. Hence, our analysis of key Deep PG primitives motivates the performance improvement of VFS-based algorithms. Appendix D shows the same analysis for VFS-DDPG and VFS-TD3, confirming our results.

5 Related Work

Ensemble methods have been used to improve policy performance in Deep RL (He et al., 2022; Lee et al., 2021; Yang et al., 2022; Wu & Li, 2020; Ren et al., 2021) combining the predictions of multiple learning models. However, the benefits of these approaches over population-based ones are unclear, as the multiple training actors (or/and critics) introduce a significant memory footprint and non-negligible overhead at training and inference time. In addition, weighting the importance of the predictions effectively is not straightforward. Hence, ensemble algorithms in Deep RL are unsuitable for: (i) deployment on-device where memory is limited, (ii) real-time systems where inference time is crucial, or (iii) training high-dimensional DNNs where parallel computation may not be possible.

[5] Although it is possible to obtain an empirical estimate of the true gradient to further improve Deep PG performance, this would require orders of magnitude more samples than the ones used in practical applications. Using such an amount of samples is unfeasible due to the computational demands (Ilyas et al., 2020).

In contrast, population-based approaches are straightforward to implement and have been used to combine the exploration benefits of gradient-free approaches and gradient-based algorithms (Khadka & Tumer, 2018; Marchesini et al., 2021; Sigaud, 2022) for policy parameters search. In more detail, ERL (Khadka & Tumer, 2018) employs a Deep PG agent and a concurrent population that includes the gradient-based agent to explore different policy permutations. The agent trains following its gradient-based algorithm and shares a memory buffer with the population to learn from more diversified samples. However, ERL's dropout-like permutations bias the population's performance in the long run. Inspired by ERL, many policy search approaches emerged in the literature (Colas et al., 2018; Bodnar, 2020; Aloïs Pourchot, 2019; Marchesini et al., 2021). In more detail, GEP-PG (Colas et al., 2018) uses a curiosity-driven approach to enhance the experiences in the agent's memory buffer. Moreover, Proximal Distilled ERL (PDERL) (Bodnar, 2020) introduces novel gradient-based permutations to address destructive behaviors of biologically-inspired perturbations that could cause catastrophic forgetting (Lehman et al., 2018). Finally, Super-RL (Marchesini et al., 2021) combines the intuitions of the previous population-based approaches, proposing a framework applicable to (possibly) any DRL algorithms that do not exhibit detrimental policy behaviors. However, due to their policy-oriented nature, these approaches assume a simulated environment to evaluate the perturbed policies, which increases the sample inefficiency of Deep RL algorithms. Such additional interactions are also task-specific as they have to cover a broad spectrum of behaviors to ensure a robust evaluation. As discussed in Marchesini et al. (2021), such behavior diversity is crucial to ensure that a perturbed policy improves the original actor, not only in particular environment initializations. In addition, recent policy search methods introduce gradient-based perturbation (that has a non-negligible overhead, as further discussed in Section 2) to ensure that the population's predictions do not drastically diverge from the original policy. To summarize, population-based searches address the issues of ensemble methods by exploring different behaviors for the policies but disregarding value networks.

6 Discussion

Ilyas et al. (2020) recently showed that critics employed in Deep PG algorithms for value predictions poorly fit the actual return, limiting their efficacy in reducing gradient estimate variance and driving policies toward sub-optimal performance (Fujimoto et al., 2018). Despite improving Deep PG performance, population-based search methods have recently superseded ensemble learning due to their computational benefits. However, these approaches typically lack practical investigations to understand their improvement. Moreover, previous population search frameworks have been devoted to exploring policy perturbations, disregarding critics and their crucial role in Deep PG.

To our knowledge, VFS is the first gradient-free population search approach to enhance critics and improve performance and sample efficiency. Crucially, VFS can be applied to (possibly) any Deep PG algorithm and aims at finding a set of weights that minimize the same critic objective. Moreover, our detailed analysis of PG primitives in Section 4.3 motivates the performance improvement of the gradient-based agent due to VFS. In addition, such analysis suggests that the gap between the underlying theoretical framework of Deep PG and the actual tricks driving their performance may not be as significant as previously discussed (Ilyas et al., 2020). Hence, VFS opens up several exciting research directions, such as investigating the theoretical relationships between RL and practical Deep RL implementation. Another exciting trend would be to extend the analysis of Deep PG primitives to state-of-the-art algorithms to understand the relevant components driving Deep PG performance. Empirically, VFS also paves the way for novel combinations with policy search methods to provide a unified framework of gradient-free population-based approaches.

6.1 Conclusion

VFS introduces a two-scale perturbation operator voted to diversify the population of value networks to (i) explore local variations of current critics' predictions and (ii) allow to explore diversified value functions to escape from local optima. The practical results of such components have been investigated with additional experiments that also motivate the improvement in sample efficiency and performance of VFS-based algorithms in a range of common continuous control benchmarks. Overall, our findings suggest that improving fundamental Deep PG primitives effectively translates into higher-performing policies and better sample efficiency.

7 ETHICS STATEMENT

The proposed Value Function Search does not focus on experiments involving human subjects and does not require sensitive data that involve sex, gender, and diversity analysis. Hence, we do not consider the gender dimension, privacy, data governance issues, or any primary ethic concern highlighted in the *ICLR Code of Ethics*[6] to be relevant.

However, according to the *"Ethics Guidelines for Trustworthy Artificial Intelligence"* report published by the High-Level Expert Group on AI of the European Commission,[7] ethical consideration has to take into account the environment and the sustainability of AI systems. Regarding the environmental impact, it is crucial to foster sample efficiency (i.e., reducing the training time for the agents, hence the computational resources used to train them) of Deep RL to lower energy consumption and related emissions. In this direction, VFS leads to significant benefits in sample efficiency, which reduces the environmental footprint of VFS-based approaches by a considerable margin.

In more detail, we employed the Machine Learning CO2 impact calculator (Lacoste et al., 2019) to estimate the CO2 emissions of our experiments.[8] According to our hardware, the carbon efficiency of the provider, and the length of our experiments, we computed a total emission of ≈ 52.3 kg CO2. We plan to cope with such emissions using Treedom[9], an online service that allows us to plant trees to cope with our carbon footprint.

8 REPRODUCIBILITY STATEMENT

Significant efforts have been made to ensure the reproducibility of VFS. Section 3 detail the flow of VFS-based algorithms with pseudocode and detailed explanations. We also highlight possible limitations of our approach in Section 3.1. Moreover, Section 4 states our experimental setup, while supplemental material contains a detailed overview of the considered hyperparameters.

To ensure reproducibility, we will release an anonymized version of our code during the discussion period to keep it visible only to the reviewers and ACs before publication (as indicated in the ICLR author's guide).

[6] https://iclr.cc/public/CodeOfEthics

[7] https://digital-strategy.ec.europa.eu/en/library/ethics-guidelines-trustworthy-ai

[8] We note that this is not a precise measurement as it is not trivial to map energy consumption to CO2 emissions (i.e., the carbon footprint). To this end, we employed open-source electricity maps (e.g., https://www.electricitymaps.com) to better estimate how carbon-intensive our experiment's electricity is.

[9] https://www.treedom.net

REFERENCES

Olivier Sigaud Aloïs Pourchot. CEM-RL: Combining evolutionary and gradient-based methods for policy search. In *International Conference on Learning Representations (ICLR)*, 2019.

Pietro Lio' Bodnar, Ben Day. Proximal distilled evolutionary reinforcement learning. In *Conference on Artificial Intelligence (AAAI)*, 2020.

Greg Brockman, Vicki Cheung, Ludwig Pettersson, Jonas Schneider, John Schulman, Jie Tang, and Wojciech Zaremba. Openai gym. *OpenAI*, 2016.

Cédric Colas, Olivier Sigaud, and Pierre-Yves Oudeyer. GEP-PG: decoupling exploration and exploitation in deep reinforcement learning algorithms. In *International Conference on Machine Learning (ICML)*, 2018.

Cédric Colas, Olivier Sigaud, and Pierre-Yves Oudeyer. A hitchhiker's guide to statistical comparisons of reinforcement learning algorithms. *arXiv*, 2019.

Scott Fujimoto, Herke van Hoof, and David Meger. Addressing function approximation error in actor-critic methods. In *International Conference on Machine Learning (ICML)*, 2018.

Tuomas Haarnoja, Aurick Zhou, Pieter Abbeel, and Sergey Levine. Soft actor-critic: Off-policy maximum entropy deep reinforcement learning with a stochastic actor. In *International Conference on Machine Learning (ICML)*, 2018.

Qiang He, Huangyuan Su, Chen GONG, and Xinwen Hou. MEPG: A minimalist ensemble policy gradient framework for deep reinforcement learning. In *Decision Awareness in Reinforcement Learning Workshop at ICML 2022*, 2022.

Peter Henderson, Riashat Islam, Philip Bachman, Joelle Pineau, Doina Precup, and David Meger. Deep reinforcement learning that matters. In *Conference on Artificial Intelligence (AAAI)*, 2018.

Andrew Ilyas, Logan Engstrom, Shibani Santurkar, Dimitris Tsipras, Firdaus Janoos, Larry Rudolph, and Aleksander Madry. A closer look at deep policy gradients. In *International Conference on Learning Representations (ICLR)*, 2020.

Shauharda Khadka and Kagan Tumer. Evolutionary reinforcement learning. In *Advances in Neural Information Processing Systems (NeurIPS)*, 2018.

Shauharda Khadka, Somdeb Majumdar, Tarek Nassar, Zach Dwiel, Evren Tumer, Santiago Miret, Yinyin Liu, and Kagan Tumer. Collaborative evolutionary reinforcement learning. In *International Conference on Machine Learning (ICML)*, 2019.

Alexandre Lacoste, Alexandra Luccioni, Victor Schmidt, and Thomas Dandres. Quantifying the carbon emissions of machine learning. *CoRR*, 2019.

Kimin Lee, Michael Laskin, Aravind Srinivas, and Pieter Abbeel. Sunrise: A simple unified framework for ensemble learning in deep reinforcement learning. In *International Conference on Machine Learning (ICML)*, 2021.

Joel Lehman, Jay Chen, Jeff Clune, and Kenneth O. Stanley. Safe mutations for deep and recurrent neural networks through output gradients. In *GECCO*, 2018.

Timothy P. Lillicrap, Jonathan J. Hunt, Alexander Pritzel, Nicolas Heess, Tom Erez, Yuval Tassa, David Silver, and Daan Wierstra. Continuous control with deep reinforcement learning. In *International Conference on Learning Representations (ICLR)*, 2016.

Enrico Marchesini, Davide Corsi, and Alessandro Farinelli. Genetic soft updates for policy evolution in deep reinforcement learning. In *International Conference on Learning Representations (ICLR)*, 2021.

Josè Antonio Martin H. and Javier de Lope. Learning autonomous helicopter flight with evolutionary reinforcement learning. *Computer Aided Systems Theory*, 2009.

Jie Ren, Yewen Li, Zihan Ding, Wei Pan, and Hao Dong. Probabilistic mixture-of-experts for efficient deep reinforcement learning. *arXiv*, 2021. openreview.net/forum?id=LtgEkhLScK3.

John Schulman, Sergey Levine, Philipp Moritz, Michael I. Jordan, and Pieter Abbeel. Trust region policy optimization. In *International Conference on Machine Learning (ICML)*, 2015.

John Schulman, Filip Wolski, Prafulla Dhariwal, Alec Radford, and Oleg Klimov. Proximal policy optimization algorithms. *arXiv*, 2017.

Olivier Sigaud. Combining evolution and deep reinforcement learning for policy search: a survey. *arXiv*, 2022.

David Silver, Guy Lever, Nicolas Heess, Thomas Degris, Daan Wierstra, and Martin Riedmiller. Deterministic policy gradient algorithms. In *International Conference on International Conference on Machine Learning (ICML)*, 2014.

Richard S. Sutton and Andrew G. Barto. *Reinforcement Learning: An Introduction*. The MIT Press, 2018.

Richard S. Sutton, David McAllester, Satinder Singh, and Yishay Mansour. Policy gradient methods for reinforcement learning with function approximation. In *Advances in Neural Information Processing Systems (NeurIPS)*, 1999.

Emanuel Todorov, Tom Erez, and Yuval Tassa. Mujoco: A physics engine for model-based control. In *IEEE/RSJ International Conference on Intelligent Robots and Systems (IROS)*, 2012.

Christopher Watkins and Peter Dayan. Q-learning. *Machine Learning*, 8:279–292, 1992.

M. A. Wiering and H. van Hasselt. Ensemble algorithms in reinforcement learning. *Trans. Sys. Man Cyber. Part B*, 38(4), 2008.

Ronald J Williams. Simple statistical gradient-following algorithms for connectionist reinforcement learning. *Machine Learning*, 8:229–256, 1992.

Junta Wu and Huiyun Li. Deep ensemble reinforcement learning with multiple deep deterministic policy gradient algorithm. *Mathematical Problems in Engineering*, 2020.

Zhengyu Yang, Kan Ren, Xufang Luo, Weiqing Liu, Jiang Bian, Weinan Zhang, and Dongsheng Li. Deep ensemble policy learning. *arXiv*, 2022. openreview.net/forum?id=-7NOEQcD-xH.

A EFFECTS OF PERTURBATIONS ON VFS-PPO, VFS-DDPG, VFS-TD3

Figure 5 reports the missing experiments in Section 4.1 regarding the effects of our perturbations at different stages of the training (i.e., at 100k, 500k, 1M steps) for VFS-PPO, VFS-DDPG, VFS-TD3.

Figure 5: Efficacy of the $\sigma_{min,max}$ scales in modifying PPO (on the first row), DDPG (on the second row), and TD3 (on the third row) critics to achieve similar predictions or more diversified ones to escape local optima, respectively.

Similarly to the evaluation in Section 4.1, the values of the σ_{min} perturbed critic differ from the original critic by a small margin. In contrast, the value network perturbed with σ_{max} has significantly different values. Interestingly, our experiments with different algorithms consider the same

set of hyperparameters for the mutation operators (see Appendix E), suggesting that VFS does not require extensive tuning to enhance existing Deep PG algorithms.

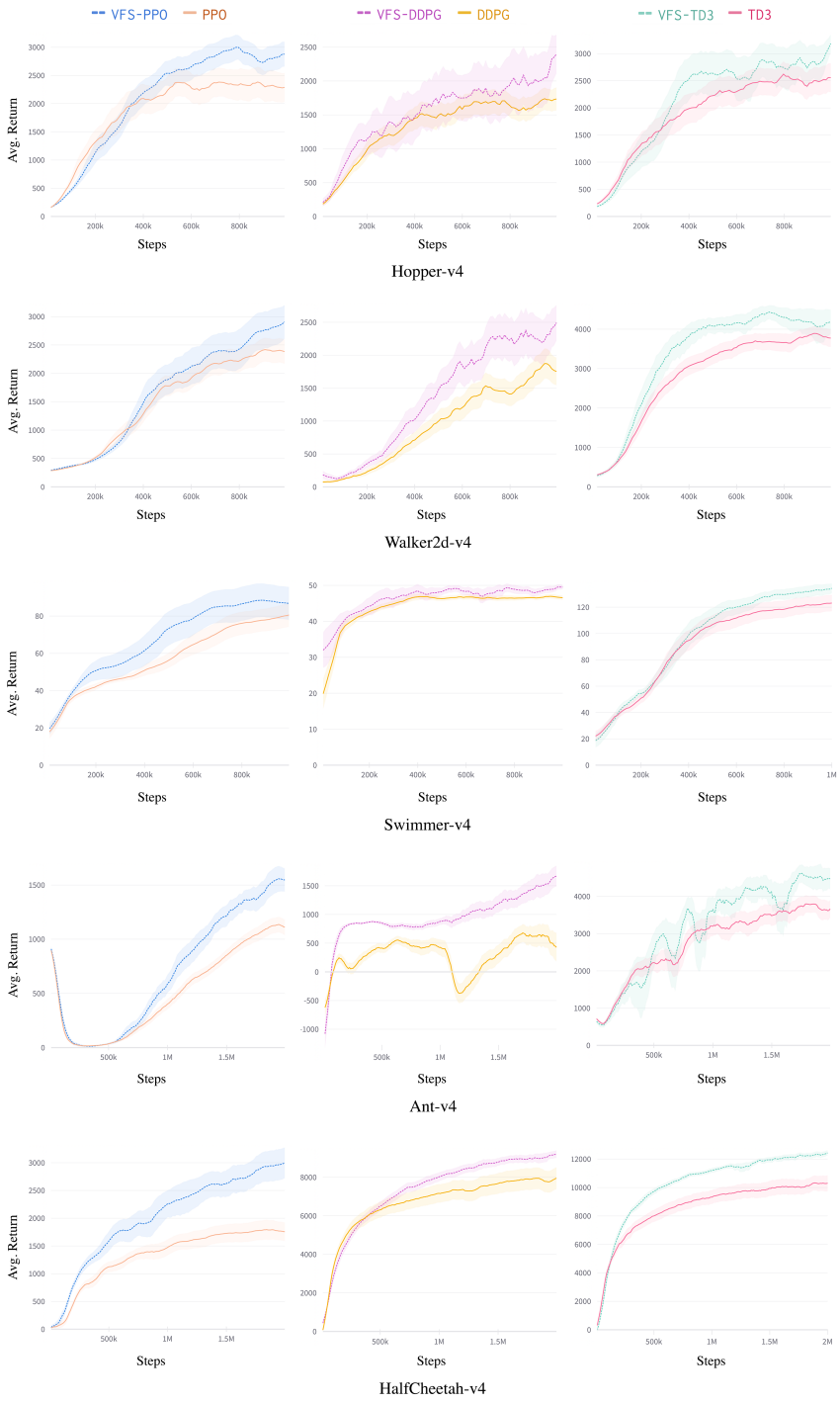

Figure 6: Comparison of PPO, DDPG, TD3, and their VFS implementation in common continuous control benchmarks on each row. Each column (i.e., each couple of algorithms) shows the average return during the training over 25 runs. VFS-based implementations improve average return and sample efficiency of the baseline Deep PG algorithms.

B TRAINING CURVES

Following the results in Section 4.2, Figure 6 shows the average return during the training. We report the results for each environment in the different rows, while each column contains a different set of algorithms (i.e., VFS-PPO and PPO in the first column, VFS-DDPG and DDPG in the second column, VFS-TD3 and TD3 in the last one). As discussed in the main paper, VFS-based algorithms achieve, on average, higher returns with lower standard deviation. Moreover, they significantly improve sample efficiency, reaching the peak performance of the baseline algorithms (i.e., PPO, DDPG, TD3) in a fraction of the steps.

C ADDITIONAL EXPERIMENTS

In this section, we discuss the computation overhead of ensemble methods and population-based ones. Moreover, we report additional experiments with VFS-PPO in the Hopper environment to show the influence of different population sizes on performance and the lower results achieved by annealing the perturbations.

C.0.1 COMPUTATION OVERHEAD

In this section, we compare the overhead of training and inference time introduced by Supe-RL, SUNRISE, and VFS, considering $M = 10$ models. The training overhead is comparable for all the approaches as common Deep RL benchmarks do not require high-dimensional DNNs or computational demanding architectures that hinder parallelization. Nonetheless, in more complex tasks requiring high-dimensional DNNs, it could be computationally unfeasible to parallelize the training models of ensemble methods, especially during backpropagation. As reported by the Supe-RL's authors (Marchesini et al., 2021), the additional environments interactions of policy search methods lead to a maximum 6% overhead even considering parallelization with a population of size M. In contrast, VFS does not require multiple training models or additional environment interactions, leading to a negligible overhead for the training procedure (i.e., it simply requires additional forward DNNs propagations).

Regarding inference time, policy and value network searches do not involve multiple predictions (except in the periodical search, which has negligible overhead due to batched computations), maintaining the same inference time of the original Deep PG baselines. In contrast, as detailed by SUNRISE's authors (Lee et al., 2021), their ensemble agents require up to $2M\times$ additional inference time.

To summarize, gradient-free search methods are generally less computationally demanding than ensemble ones. Hence, the superior return of VFS, sample efficiency, and computational benefits further confirm the merits of introducing a critics' search-based approach.

C.0.2 POPULATION SIZE AND ANNEALING RESULTS

Figure 7 on the left shows the performance with increasing sizes for the population (i.e., 4, 8, 12, 20). Intuitively, increasing the size of the population leads to higher performance. However, our experiments show no significant advantage in considering a population of size greater than 10 (the one used in our experiments in the main paper).

Figure 7 on the right shows the comparison between PPO, VFS-PPO, and VFS-PPO with annealing on the perturbations. In more detail, we linearly scale the effects of the perturbations to zero towards step 900k. As discussed in Section 3, after zeroing out VFS's perturbations, our approach is equivalent to the considered Deep PG baseline and, as such, has the same convergence guarantee in the limit. Nonetheless, in practice, VFS-PPO without permutation annealing achieves superior performance as the critic's population search keeps improving the Deep PG primitives.

D ADDITIONAL DEEP PG PRIMITIVES ANALYSIS

In Section 4.3, we analyzed the improvement of VFS-PPO in terms of gradient estimate, their variance, and the mean squared error of the critic. Such analysis serves to motivate the performance

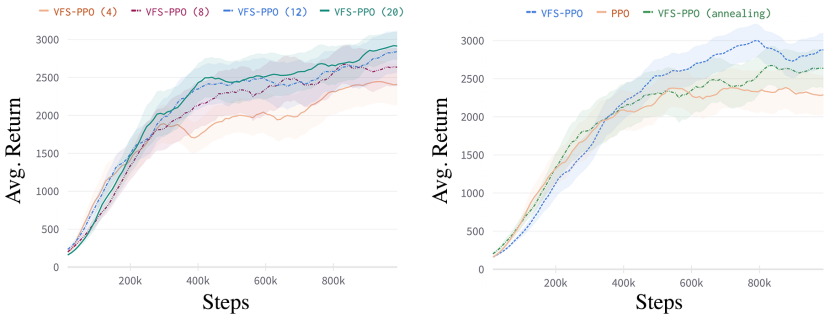

Figure 7: Left: influence of different population sizes in VFS-PPO. Empirical evidence shows that increasing the size of the population leads to higher performance. Right: comparison between PPO, VFS-PPO, and VFS-PPO with annealing perturbations. Linearly scaling our perturbations to zero leads to lower performance with respect to the proposed VFS-PPO with fixed permutations.

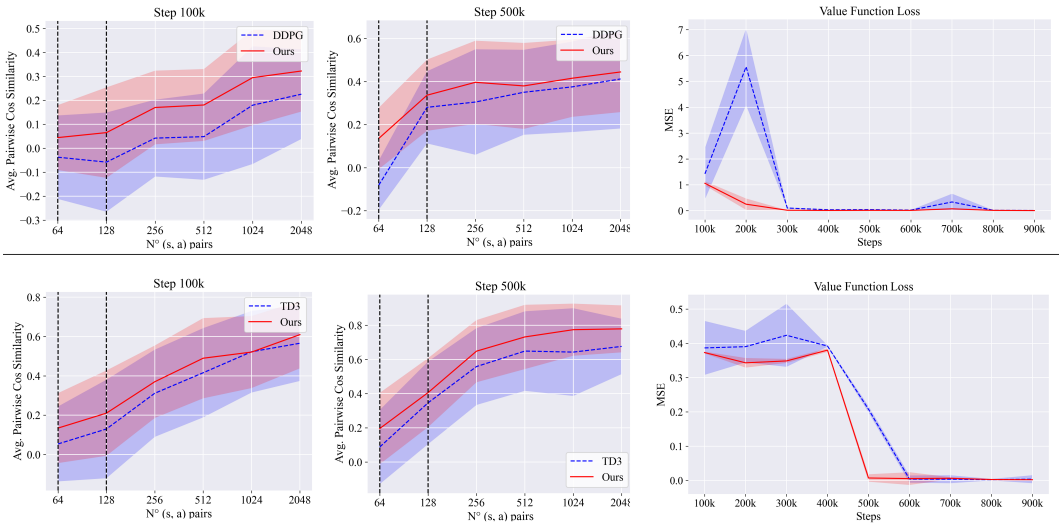

Figure 8: Analysis of gradient estimate and variance (left, middle) in the Hopper task for DDPG and VFS-DDPG in the first row, TD3 and VFS-TD3 in the second row. We measure the average pairwise cosine similarity (y-axis) between 30 gradient estimates which use a growing number of state-action pairs (x-axis). For each algorithm, we use the average over the 25 models collected during the training runs at 10^5 and 5×10^5 steps. The higher correlation with a lower variance of VFS-based implementations translates into better performance of the Deep PG algorithm. Average MSE of such models over the training phase (right).

improvement of VFS-based algorithms. In this section, we report the same comparison for VFS-DDPG and VFS-TD3 to further confirm the benefits of the proposed framework.

Figure 8 reports the same results for our Deep PG primitives analysis for DDPG and TD3. We measure the average pairwise cosine similarity and its standard deviation between 30 gradient measurements taken from the algorithms at 10^5 and 5×10^5 steps in the Hopper task with an increasing number of state-action pairs. Crucially, VFS-DDPG and VFS-TD3 show a higher correlation and lower variance in the typical sampling regime used during the training (i.e., mini-batches of size 64 or 128), motivating their performance improvement over the baselines. Moreover, the right column shows the average MSE of our models computed every 10^5 step. Results follow the trend of Section 4.3, where VFS critics have lower MSE. Interestingly, we also note that TD3 typically achieves a higher gradient estimate correlation with lower variance over DDPG, which motivates its use of two value networks to achieve better performance. To summarize, our analysis of key Deep PG primitives for DDPG and TD3 confirms the main paper's results.

E HYPERPARAMETERS

We performed an initial grid search among common hyper-parameters from prior work (Schulman et al., 2017; Lillicrap et al., 2016; Fujimoto et al., 2018; Marchesini et al., 2021). This evaluation led us to use similar DNN architectures for all the algorithms in the environments, i.e., 2-ReLU layer MLP with 64 hidden units each to model actors, and critics for PPO, and the same structure but with 256 hidden units for DDPG, TD3. Table 2 reports the other hyperparameters shared across all the experiments. Note that missing parameters are the same as the baseline algorithm (e.g., VFS-PPO values are the same as PPO, and TD3 shares the missing parameters with DDPG). Moreover, all the VFS-based implementations consider the same values for the critic's search.

Table 2: Hyperparameters for our experiments

Algorithm	**Parameter**	**Value**
PPO	ϵ clip	0.2
	γ	0.99
	update epochs	10
	samples per update	2048
	mini-batch size	64
	entropy coefficient	0.001
	lr	0.0003
DDPG	γ	0.99
	buffer size	1000000
	mini-batch size	128
	actor lr	0.0001
	critic lr	0.001
	τ	0.005
TD3	actor noise clip	0.5
	delayed actor update	2
VFS	population size	10
	σ_{min}	0.000005
	σ_{max}	0.0005
	b	2048